

# Leidenfrost on a ratchet

Guillaume Lagubeau<sup>1,2†</sup>, Marie Le Merrer<sup>1,2†</sup>, Christophe Clanet<sup>1,2</sup> and David Quéré<sup>1,2\*</sup>

**As discovered by Leidenfrost, liquids placed on very hot solids levitate on a cushion of their own vapour<sup>1–3</sup>. These model hovercrafts are remarkably mobile: placed on a hot ratchet, a droplet not only levitates, but also self-propels, in a well-defined direction, at a well-defined velocity<sup>4</sup> (typically,  $10 \text{ cm s}^{-1}$ ). The challenge is to understand the origin of the phenomenon, which contrasts with other situations where an asymmetry in the solid/liquid contact was used to generate liquid self-propulsion<sup>5–15</sup>. We consider Leidenfrost solids that directly sublime on hot substrates, and show that they also self-propel on ratchets. This leads to a scenario for the motion: the vapour flow escaping below the Leidenfrost body gets rectified by the presence of asymmetric textures, so that a directional thrust drives the levitating material. Using fishing lines to catch drops, we measure the force acting on them, and discuss both the driving force and the special friction generated by the textures.**

Self-propelling fluidic devices have received special attention over the past few years because of their unique ability to displace liquid at small scales without an external force. These devices can be used to chemically treat a solid<sup>5–8</sup>, to direct and concentrate liquid, for example in condensers<sup>9</sup>, or to drive compounds, as observed with the phalarope, a bird that drives its prey mouthward encapsulated in water<sup>15</sup>. In a self-propelling situation, asymmetry is the primary cause of motion. This asymmetry can be provided by a contrast in wettability, possibly maintained by a chemical reaction, a temperature gradient or geometrical effects<sup>10–15</sup>. However, the resulting capillary force is comparable to the sticking force arising from the presence of defects on the solid, so that motion must often be triggered by injecting energy into the system, using vibrations for example<sup>16–18</sup>.

In this context, the system discovered in 2006 by Linke *et al.* is particularly appealing<sup>4</sup>. There the authors considered Leidenfrost non-stick drops levitating on hot solids, in the film-boiling regime<sup>19</sup>, and showed that these drops self-propel if asymmetric teeth are present on the solid. The teeth have millimetric lengths and heights of typically  $150 \mu\text{m}$ . The solid is heated well above the Leidenfrost temperature at which the vapour film builds up, so that the tips of the teeth do not induce boiling. Drops on these hot ratchets accelerate and reach a constant velocity of the order of  $5\text{--}15 \text{ cm s}^{-1}$  (ref. 4). They follow the direction such that they climb the steps, as seen in Fig. 1. The motion is observed provided that the drop is larger than the tooth size: here we mainly consider drops with radii between 3 mm and 1 cm, for which the liquid is flattened by gravity, as observed in Fig. 1.

Many effects can *a priori* be responsible for the propulsion, as guessed from Fig. 1. First, the base of the drop is deformed by the presence of the ratchet below, which induces a modulation of its curvature and consequent Laplace pressure gradients<sup>4</sup>. Second, a wave propagates from the trailing edge to the leading edge

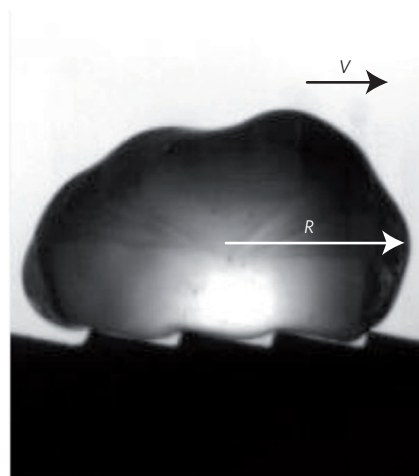


**Figure 1 | The device of Linke *et al.*** A drop deposited on a hot ratchet (of temperature much higher than the boiling temperature of the liquid, so that a vapour film separates the solid from the liquid) self-propels in the direction indicated by the arrow. Here the drop has an equatorial radius  $R = 3 \text{ mm}$ . The ratchet is made of brass and brought to a temperature  $T = 350 \text{ }^\circ\text{C}$ , much greater than  $200 \text{ }^\circ\text{C}$ , the Leidenfrost temperature for ethanol, at which boiling would be observed. The teeth have a length of  $1.5 \text{ mm}$  and a height of  $300 \mu\text{m}$ . After a short transient regime of acceleration, the drop moves at a constant velocity  $V = 14 \text{ cm s}^{-1}$ .

of the drop, making the transport of matter possible in the direction of its motion. Third, a Leidenfrost drop is likely to oscillate spontaneously<sup>20</sup>; for each elementary rebound, part of the kinetic energy can be transferred from the vertical to the horizontal direction because of the slope of the teeth. Fourth, the Marangoni effect related to temperature differences might cause a displacement, as seen in Marangoni-levitating drops heated asymmetrically using a light source<sup>21</sup>. Fifth, as the drop loses material, this gas flow might provoke a motion provided it is made directional (or rectified) by the presence of the teeth.

It is crucial to note that the first four possibilities above are related to the deformability of the moving body, that is, to its liquid nature; hence the question arises whether a motion is still possible using a levitating solid instead of a liquid. It turns out that one solid is particularly suitable for such an experiment: so-called dry ice, which is solid carbon dioxide, has the property to sublime at atmospheric pressure. The sublimation point is  $-78.5 \text{ }^\circ\text{C}$ , and the ice density is  $1,500 \text{ kg m}^{-3}$ . We modelled disks of dry ice, the centimetric radii and millimetric thicknesses of which are comparable to those of drops. These disks were deposited on the hot ratchet ( $T = 350 \text{ }^\circ\text{C}$ ) used previously, producing the effects shown in Fig. 2.

<sup>1</sup>Physique et Mécanique des Milieux Hétérogènes, UMR 7636 du CNRS, ESPCI, 75005 Paris, France, <sup>2</sup>Ladhyx, UMR 7646 du CNRS, École Polytechnique, 91128 Palaiseau Cedex, France. <sup>†</sup>These authors contributed equally to this work. \*e-mail: david.quere@espci.fr

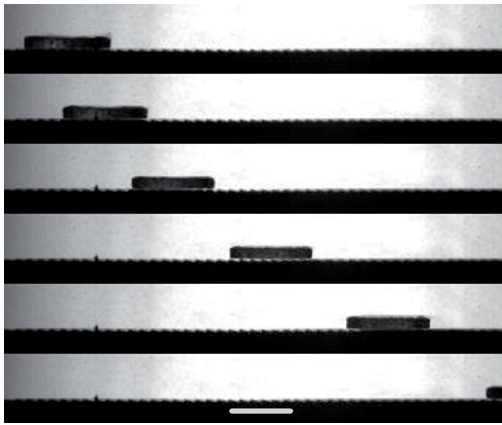


**Figure 2 | Dry ice propulsion.** Disk (millimetric thickness, centimetric diameter) of solid carbon dioxide on a hot ratchet ( $T = 350^\circ\text{C}$ ): this Leidenfrost solid (the dry ice directly sublimates), starting from rest (first picture), self-propels, as observed for a liquid, and in the same direction. The bar indicates one centimetre and the time interval between two successive photos is 300 ms.

Dry ice indeed levitates and moves in the same direction as Leidenfrost drops (see Fig. 1). The ice disk is driven by a constant force, as deduced from the constant acceleration in this start up regime. Hence, even Leidenfrost solids self-propel on hot ratchets, implying that the motion is not necessarily related to liquid surface deformation. We can thus assume vapour production to be the primary cause of motion. Whereas vapour escapes in an isotropic way on a flat solid, its flow can be made anisotropic by the presence of a ratchet. For typical values of the different parameters (gas density  $\rho \sim 1\text{ kg m}^{-3}$ , viscosity  $\eta \sim 10^{-5}\text{ Pa s}$ , radial escape velocity  $U \sim 1\text{ m s}^{-1}$  and film thickness  $h$  of  $100\text{ }\mu\text{m}$  (refs 1–3)) the Reynolds number  $\text{Re} = \rho U h / \eta$  is of the order of 10, so that there is no time reversibility as the gas flows. As a consequence, this flow can be asymmetric, as known in hydraulics in the context of singular pressure loss: fluid flows are not symmetric when entering a sudden contraction or emerging from it<sup>22</sup>. As the gas moves towards the step, that is towards a sudden contraction in the fluid channel, the flow resistance is higher than in the reverse direction<sup>23</sup>. As a consequence, the vapour will mainly escape along the smallest slopes of the texture, which propels the Leidenfrost body in the direction shown in Figs 1 and 2 (jet thrust). This interpretation was confirmed by forcing contact between the hot ratchet and a disk of dry ice, thus printing the tooth pattern on the bottom of the disk, and observing a similar motion with this textured disk on a hot flat solid. Note that the size  $R$  of the moving object is assumed larger than the tooth length, so that an asymmetric vapour flow can indeed occur—a condition emphasized as being necessary to observe motion<sup>4</sup>.

If  $\dot{M}$  is the mass of gas ejected per unit time, the force propelling the object will scale as  $\dot{M}\Delta U$ , where  $\Delta U$  is the difference of gas velocity between the two directions. This quantity will depend on the exact shape of the teeth (the more symmetric they are, the smaller  $\Delta U$ ) and on the ratio between the film thickness  $h$  and the step height (the larger  $h$ , the smaller the effect of the ‘channel constrictions’, and thus the smaller  $\Delta U$ ). As we expect  $\Delta U$  to scale as  $U$ , we shall write  $\Delta U = \alpha U$ , where the number  $\alpha$  describes the degree of flow asymmetry<sup>22</sup>. In our case,  $h$  is smaller than the step height and the teeth are very asymmetric, so that we expect  $\alpha$  to be of order unity. It should be noted that some of the gas escapes laterally and does not contribute to the propulsion. This three-dimensional effect will reduce the numerical coefficient in the law of propulsion, but will not affect the scaling laws.

To obtain a more quantitative understanding of the driving force  $F_0$  and how it varies with the drop size, we need to evaluate both  $\dot{M}$  and the radial gas velocity  $U$ . We consider a large Leidenfrost drop flattened by gravity, such that the base radius can be identified with the equatorial radius  $R$  defined in Fig. 1. The drop floats on a vapour cushion of thickness  $h$ , and conservation of matter can be written as:

$$\dot{M} \sim \rho h R U \quad (1)$$

The amount of matter evaporated per unit time results from a classical energy balance. After a short transient regime (generally smaller than 1 s), the temperature of a Leidenfrost body reaches its boiling temperature, so that further heat supplied by the substrate is mainly used to drive the phase change: in this stationary regime, the temperature difference  $\Delta T$  between the solid and the liquid is constant. It has been shown that conduction dominates the heat transfer<sup>2</sup>, so the energy balance can be written per unit time as:

$$\dot{M} L \sim (\kappa \Delta T / h) R^2 \quad (2)$$

where we denoted the thermal conductivity of the vapour as  $\kappa$  and the latent heat of evaporation as  $L$ . In addition, we assume that thermal exchanges and evaporation mainly take place on the surface area  $R^2$  facing the hot solid. Furthermore, a Leidenfrost body of height  $H$  and density  $\rho_0$  squeezes the film by imposing a pressure  $\rho_0 g H$ . In the lubrication approximation ( $h \ll R$ ), the resulting flux is:

$$\dot{M} \sim (\rho h^3 / \eta) \rho_0 g H \quad (3)$$

The stationary vapour film is fed by evaporation at the rate at which vapour escapes<sup>2,3</sup>. Equations (2) and (3) can be equated, which yields a relationship between the film thickness  $h$  and the drop radius  $R$ :

$$h \sim a^{1/2} R^{1/2} \quad (4)$$

with  $a = (\kappa \eta \Delta T / L \rho \rho_0 g H)^{1/2}$ . For drops larger than the capillary length, the liquid thickness  $H$  becomes independent of the drop size and is set by the capillary length, that is, a few millimetres for ordinary liquids. Typical values for the other parameters are:  $\kappa \approx 0.03\text{ W m}^{-1}\text{ K}^{-1}$ ,  $\eta \approx 2 \times 10^{-5}\text{ Pa s}$ ,  $L \approx 10^6\text{ J kg}^{-1}$ ,  $\rho \approx 10^3\text{ kg m}^{-3}$  and  $\rho_0 \approx 10^3\text{ kg m}^{-3}$ . Hence, we find  $a \approx 3\text{ }\mu\text{m}$ , which, for radii  $R$  of a few millimetres, yields a film thickness  $h$  on the order of  $100\text{ }\mu\text{m}$ , as observed experimentally<sup>3</sup>. Combining equations (3) and (4) gives the  $\dot{M}(R)$  variation:

$$\dot{M} \sim \rho a^{3/2} R^{3/2} / \tau \quad (5)$$

where  $\tau = \eta / \rho_0 g H$  is the characteristic viscous relaxation time of the film associated with an applied pressure of  $\rho_0 g H$ —a time of the order of  $1\text{ }\mu\text{s}$ . Equation (5) shows that  $\dot{M}$  increases as  $R^{3/2}$ , so that we can express the force  $F \sim \dot{M} U$  likely to drive the drop on the ratchet. Combining equations (1), (4) and (5), and noting  $F_0 \approx \rho a^4 / \tau^2$ , we find:

$$F \sim F_0 (R/a)^{3/2} \quad (6)$$

For the values estimated above ( $a \sim 3\text{ }\mu\text{m}$  and  $\tau \sim 1\text{ }\mu\text{s}$ ),  $F_0$  is  $10^{-4}\text{ }\mu\text{N}$ . Hence, for drops of a few millimetres, we expect a propelling force  $F$  of the order of  $10\text{ }\mu\text{N}$ , which rapidly increases with the drop size  $R$ . To determine the intensity of the force  $F$  driving the motion, we placed a long (10 cm) glass fibre of diameter  $125\text{ }\mu\text{m}$  in the path of the droplet. As it moves, the drop is caught by the fibre, which gets deflected by a distance  $\delta$ , at which point the

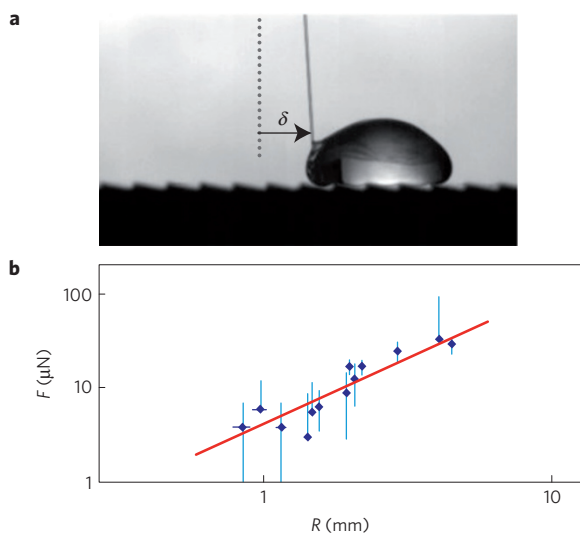


**Figure 3 | Force measurement.** **a**, A thin glass fibre placed in the drop's path catches the drop, deflecting the fibre by a distance  $\delta$ . The dotted line shows the initial position of the fibre. Previously calibrating the elastic response of the fibre allows us to measure the force  $F = K\delta$  acting on the liquid. The drop slowly evaporates, causing its equatorial radius  $R$  to decrease with time. The distance  $\delta$  also decreases, showing that  $F$  is an increasing function of  $R$ , as shown in **b**. The slope  $3/2$  drawn as a solid line suggests that  $F$ , typically  $10 \mu\text{N}$  for millimetric drops, increases as  $R^{3/2}$ . The error bars at large  $F$  indicate the amplitude of the fluctuations of the force in the experiments; at small  $F$ , the drop becomes sensitive to the discrete nature of the steps of length  $\lambda$ , so that here the error bars correspond to  $F(\delta = \lambda)$ .

drop stops (Fig. 3a). As  $F$  is being balanced there by the elastic force associated with the deflection, we can deduce quantitative values of  $F$  in this range of force. In a Leidenfrost situation, the vapour layer prevents the drops from boiling; instead, they slowly evaporate, with a typical lifetime of one minute<sup>1–3,24</sup>, allowing us to measure the force/radius relationship during this time. The drop size can be varied by one order of magnitude, from the millimetre-scale below which there is no motion, to the centimetre-scale where Leidenfrost drops become unstable because of the appearance of a central vapour bubble<sup>3</sup>. We observe in Fig. 3b that the fibre displacement  $\delta$  decreases as the drop evaporates, showing that the force  $F$  acting on the liquid increases with the size  $R$ .

In the log–log representation of Fig. 3b, the data seem to be fairly well aligned, indicating a power law relationship between  $F$  and  $R$ . The data are scattered, but the best fit provides an exponent of 1.47, close to the straight line of slope 1.5 superimposed on the data. The typical value of the force  $F$  is  $10 \mu\text{N}$  for  $R \approx 3 \text{ mm}$ , a relatively small value compared with other characteristic forces at this scale: the weight of a drop of the same volume, for example, is 10 times larger. However, this force is large enough to induce fast motion because of the low friction in the Leidenfrost situation. The order of magnitude of  $F$  and its dependence on  $R$  are found to be in good agreement with equation (6), which quantitatively supports vapour-based propulsion. For this kind of model hovercraft, evaporation provides both levitation and propulsion, which itself is made possible only by levitation: any contact with the solid surface would stop the motion, because of a contact angle hysteresis that induces a resisting force, scaling as  $\gamma R$  (with  $\gamma$  the surface tension), of the order of  $100 \mu\text{N}$ . Other effects might be invoked to explain a motion based on evaporation. Teeth could induce an asymmetric evaporation close to the tops, in the direction pointed to in Fig. 1, which yields a viscous drag  $(\eta U/h)R^2$  in the same direction. From equations (1)–(4), this drag also scales as  $R^{3/2}$  and is in the  $\mu\text{N}$  range. However, the vapour flow observed

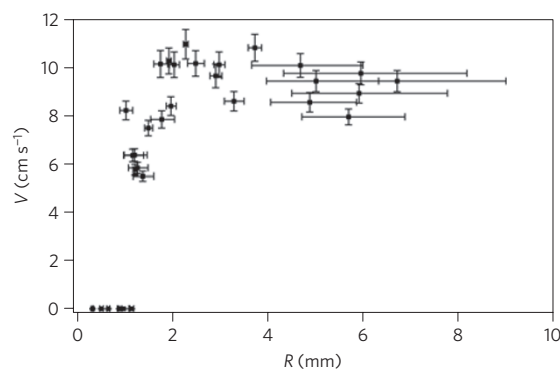


**Figure 4 | Terminal velocity of the drops.** The terminal velocity  $V$  of ethanol Leidenfrost drops on a ratchet (heated to  $T = 360^\circ\text{C}$ ) is plotted as a function of the drop equatorial radius  $R$ . The wavelength of the ratchet is  $\lambda = 1.5 \text{ mm}$ . For drops smaller than  $\lambda$ , there is no motion. For drops of radius between 2 and 7 mm, the terminal velocity varies only slightly with the drop size. The order of magnitude of this terminal velocity is  $10 \text{ cm s}^{-1}$ . The error bars at large radius correspond to the fact that the drops (flattened by gravity in this limit) rotate and vibrate, which generates an apparent change of radius as seen from the side; at small radius, the drops are more spherical, and the error bars smaller. The value of the terminal velocity  $V$  is obtained from a fit to the trajectory. The extreme fits yield the bounds of the terminal velocity, from which we deduce the error bar (typically  $\pm 0.5 \text{ cm s}^{-1}$ , much smaller than  $V$ ).

(with tracers) at the tooth scale was found to be mainly directed towards the back of the drop, which made us favour a thrust effect.

Finally, we discuss the terminal velocity of these drops. The terminal velocity  $V$  is reached after a run of a few centimetres, a distance significantly smaller than the total size of our ratchets, and is shown in Fig. 4 as a function of the drop size  $R$ . This figure clearly shows the existence of a threshold to trigger the motion: drops smaller than 1.5 mm, that is, the wavelength of the ratchet, remain immobile. This is in accord with the argument of an anisotropic vapour flow: this flow can exist only if the vapour film contacts the ratchet over more than one wavelength. For larger drops, the velocity increases quickly, reaching values as high as approximately  $10 \text{ cm s}^{-1}$ , a remarkable speed considering the weakness of the driving force. This terminal velocity  $V$  varies only slightly with the drop size  $R$  (here between 2 and 7 mm, above which a Leidenfrost drop becomes unstable). The observed tendency is a weak decrease in this interval of velocity.

Friction is generally very weak in a Leidenfrost situation. Both the viscous friction in the subjacent film, scaling as  $(\eta V/h)R^2$ , and the inertial friction related to the air displacement, scaling as  $\rho V^2 R^2$ , are of the order of  $0.1 \mu\text{N}$ , 100 times smaller than the driving force  $F$ . In the stationary regime (Fig. 4), friction and propulsion balance each other, which shows that the drop experiences a 'special' friction much larger (by two orders of magnitude) than usual. This can be understood in Fig. 1, where we see that the interface below the drop is distorted by the presence of the teeth. As the drop moves, rolls of liquid hit the steps, which dissipates energy (similarly, we checked that a Leidenfrost drop impacting a crenellated surface no longer bounces). We can evaluate the corresponding friction force: denoting by  $\lambda$  and  $\varepsilon$  the length and depth of each tooth respectively, the mass of a roll scales as  $\rho_o \lambda \varepsilon R$ . This mass decelerates in a time  $\lambda/V$ . Once integrated over the number  $R/\lambda$  of rolls, this yields for the friction force:

$$F \sim \rho_o V^2 R^2 \varepsilon / \lambda \quad (7)$$

and with  $\rho_o \approx 10^3 \text{ kg m}^{-3}$ ,  $V \approx 10 \text{ cm s}^{-1}$ ,  $R \approx 3 \text{ mm}$ , and  $\varepsilon/\lambda \approx 1/10$ , we expect a force of the order of  $10 \mu\text{N}$ , as observed

experimentally. In contrast, friction is much smaller for dry ice, which does not deform: as seen in Fig. 2, the solid continues to accelerate over distances of 10 cm, without reaching its terminal velocity.

Combining equations (5)–(7) provides the terminal velocity  $V \sim (a/\tau)(\rho/\rho_0)^{1/2}(\lambda/\varepsilon)^{1/2}(a/R)^{1/4}$  of Leidenfrost drops on ratchets. As observed in Fig. 4, the terminal velocity  $V$  is found to be rather insensitive to the drop radius ( $V \sim R^{-1/4}$ ), but it can be conveniently tuned by the design of the ratchet (because it scales as  $(\lambda/\varepsilon)^{1/2}$ ). Equation (7) indeed predicts that texturing a solid with large scale crenellations ( $\lambda \approx 1$  mm,  $\varepsilon \approx 100$   $\mu$ m) can lead to considerable friction forces: instead of decelerating over a distance  $\rho_0 R/\rho$ , as they would if the friction were classically inertial, Leidenfrost drops are expected to stop on crenellated solids over a distance  $R\lambda/\varepsilon$ , that is, in centimetres rather than metres. This implies that textured solids, shown to self-propel drops if the texture is asymmetric, become impressively efficient at stopping drops if the texture is symmetric, achieving efficient traps for the ultra-mobile Leidenfrost drops.

Received 30 July 2010; accepted 14 January 2011; published online 20 February 2011

## References

1. Leidenfrost, J. G. *De Aquae Communis Nonnullis Qualitatibus Tractatus* (Duisburg, 1756).
2. Gottfried, B. S., Lee, C. J. & Bell, K. J. Leidenfrost phenomenon—film boiling of liquid droplets on a flat plate. *Int. J. Heat Mass Trans.* **9**, 1167–1172 (1966).
3. Bianco, A. L., Clanet, C. & Quéré, D. Leidenfrost drops. *Phys. Fluids* **15**, 1632–1637 (2003).
4. Linke, H. *et al.* Self-propelled Leidenfrost droplets. *Phys. Rev. Lett.* **96**, 154502 (2006).
5. Chaudhury, M. K. & Whitesides, G. M. How to make water run uphill. *Science* **256**, 1539–1541 (1992).
6. Bain, C. D., Burnett-Hall, G. D. & Montgomerie, R. R. Rapid motion of liquid drops. *Nature* **372**, 414–415 (1994).
7. Domingues Dos Santos, F. & Ondařuhu, T. Free-running droplets. *Phys. Rev. Lett.* **75**, 2972–2975 (1995).
8. Sumino, Y., Magome, N., Hamada, T. & Yoshikawa, K. Self-running droplets: Emergence of regular motion from nonequilibrium noise. *Phys. Rev. Lett.* **94**, 068301 (2005).
9. Daniel, S., Chaudhury, M. K. & Chen, J. C. Past drop movements resulting from the phase change on a gradient surface. *Science* **291**, 633–636 (2001).
10. Brochard, F. Motions of droplets on solid surfaces induced by chemical or thermal gradients. *Langmuir* **5**, 432–438 (1989).
11. De Gennes, P. G. The dynamics of reactive wetting on solid surfaces. *Physica A* **249**, 196–205 (1998).
12. Bico, J. & Quéré, D. Self-propelling slugs. *J. Fluid Mech.* **467**, 101–127 (2002).
13. Buguin, A., Talini, L. & Silberzan, P. Ratchet-like topological structures for the control of microdrops. *Appl. Phys. A* **75**, 207–212 (2002).
14. John, K., Hänggi, P. & Thiele, U. Ratchet-driven fluid transport in bounded two-layer films of immiscible liquids. *Soft Matter* **4**, 1183–1195 (2008).
15. Prakash, M., Quéré, D. & Bush, J. W. M. Surface tension transport of prey by feeding shorebirds: The capillary ratchet. *Science* **320**, 931–934 (2008).
16. Daniel, S. & Chaudhury, M. K. Rectified motion of liquid drops on gradient surfaces induced by vibration. *Langmuir* **18**, 3404–3407 (2002).
17. Shastry, A., Case, M. J. & Böhringer, K. F. Directing droplets using microstructured surfaces. *Langmuir* **22**, 6161–6167 (2006).
18. Daniel, S., Chaudhury, M. K. & de Gennes, P. G. Vibration-actuated drop motion on surfaces for batch microfluidic processes. *Langmuir* **21**, 4240–4248 (2005).
19. Tong, L. S. *Boiling Heat Transfer and Two-Phase Flow* (Taylor & Francis, 1997).
20. Snezhko, A., Ben Jacob, E. & Aranson, I. S. Pulsating-gliding transition in the dynamics of levitating liquid nitrogen droplets. *New J. Phys.* **10**, 043034 (2008).
21. Nagy, P. T. & Neitzel, G. P. Optical levitation and transport of microdroplets: Proof of concept. *Phys. Fluids* **20**, 101703 (2008).
22. Lorenceau, E., Quéré, D., Ollitrault, J. Y. & Clanet, C. Gravitational oscillations of a column in a pipe. *Phys. Fluids* **14**, 1985–1992 (2002).
23. Biswas, G., Breuer, M. & Durst, F. Back-facing step flows for various expansions at low and moderate Reynolds numbers. *J. Fluids Eng.* **126**, 362–374 (2004).
24. Wachters, L. H. J., Bonne, H. & van Nouhuis, H. J. The heat transfer from a horizontal plate to sessile water drops in the spheroidal state. *Chem. Eng. Sci.* **21**, 923–930 (1966).

## Acknowledgements

We thank A.-L. Bianco, E. Lorenceau, L. Tobin, H. Turlier, H. Rathgen, A. Le Goff, G. Dupeux and H. Wagret for stimulating discussions, and L. Quartier and D. Renard for designing the ratchets.

## Author contributions

G.L., M.L.M., C.C. and D.Q. designed the experiments; G.L. and M.L.M. carried out the experiments; G.L., M.L.M., C.C. and D.Q. developed the models; C.C. and D.Q. wrote the manuscript. G.L. and M.L.M. equally contributed to the work?

## Additional information

The authors declare no competing financial interests. Reprints and permissions information is available online at <http://npg.nature.com/reprintsandpermissions>. Correspondence and requests for materials should be addressed to D.Q.